Preprints of the 21st IFAC World Congress (Virtual)
Berlin, Germany, July 12-17, 2020

The Value Function as a Decision Support Tool in Unmanned Vehicle Operations

Miguel Aguiar [*] **João Borges de Sousa** [*] **João Miguel Dias** [**]
Jorge Estrela da Silva [***] **Américo S. Ribeiro** [**]
Renato Mendes [**,****]

[*] *LSTS, Faculty of Engineering, University of Porto, Porto, Portugal*
[**] *NMEC-CESAM, DFis, University of Aveiro, Aveiro, Portugal*
[***] *ISEP, Polytechnic Institute of Porto, Porto, Portugal*
[****] *CIIMAR, University of Porto, Porto, Portugal*

Abstract: General problems of optimal trajectory generation and of optimal space-time rendezvous for autonomous underwater vehicles affected by time-varying fluid flows are formulated and solved in the framework of dynamic programming. The optimal solutions include optimal trajectories, as well as departure times and positions.
The approach consists in using the principle of optimality (PO) to embed, for example, an optimal time to reach a target problem from some fixed position and time into a more general problem of finding the optimal time to reach a target from any point and time. The solution of this general problem is given by the value function, the solution of a Hamilton-Jacobi-Bellman equation (HJBE) which expresses the PO in an infinitesimal form. The HJBE is solved using an efficient parallel numerical solver.
The problems of interest are solved either by minimizing the value function over one or more variables (e.g., time) or by using level sets of the value function to coordinate departure times for multiple vehicles to rendezvous at a given target.
The paper presents a description and an illustration of the approach and briefly discusses how value-function-based calculations provide a very effective way to solve complex motion planning and coordination problems. The discussion is aided by examples modeling real operational scenarios using current velocity forecasts from a state-of-the-art model of the Sado river estuary in Portugal.

Keywords: Marine systems, autonomous vehicles, dynamic programming

1. INTRODUCTION

Over the two past decades, autonomous underwater vehicles (AUVs) have become a cost-effective mobile sensing platform for ocean field studies. This is due to technological advances thanks to which present day AUVs are sufficiently reliable for this purpose. Robots are also capable of collecting data at higher spatial-temporal resolutions and in previously unreachable locations (Bellingham and Rajan (2007); Wynn et al. (2014)), and multi-vehicle deployments enable new operational concepts and opportunities for data collection (Ferreira et al. (2018)).

However, these vehicles have limited operational endurance due to energy constraints. Hence, it is desirable to minimize the amount of energy expended during those phases of the mission not related to data collection, e.g. when the vehicle is commuting between its deployment location and a survey location or between two survey locations. To this end, there has been a great amount of research activity on trajectory generation methods for AUVs which take into account flow velocity forecasts produced by hydrodynamic models (Inanc et al. (2005); Rhoads et al. (2010); Lolla et al. (2014)). In some locations, such as estuaries, the speed of the currents is comparable to the maximum speed of a typical AUV, so routing vehicles through paths along which the flow velocity contributes positively to the average speed leads to energy savings.

Most research focuses on planning a trajectory given a fixed deployment time and position. When operating with reasonably small-sized and portable robots, however, the initial state (which, as the currents are time-variant, includes both the initial position and the time of deployment) can be seen as an additional degree of freedom for planning. Dynamic programming based methods (Bellman (1954)) are particularly suitable for this kind of analysis, since they provide an efficient way of computing the solution for all initial states lying inside a given departure set. That information is encoded in the value function, which provides the optimal cost to the target from any given state.

In this paper we present an innovative approach to mission planning for operations with unmanned vehicle systems, based on an implementation of an efficient numerical method Aguiar et al. (2019) which allows us to compute the value function associated to a minimum time control problem encoding complex mission constraints and objectives. In particular, we focus on two scenarios. In the first

[⋆] Corresponding author: M. Aguiar (m.ag@fe.up.pt)

Copyright lies with the authors

scenario, we consider how these value functions can be used to plan the optimal deployment time and position in a single-vehicle mission. The second scenario concerns the selection of the deployment times and positions for a set of n vehicles to rendezvous at a given target.

The rest of the paper is structured as follows: in Section 2 we briefly review existing literature in optimal trajectory planning for autonomous underwater vehicles, and describe the method we have proposed in previous work. Sections 3 and 4 discuss the use of value functions to plan the deployment time and position of a single vehicle, and the synchronized arrival of two vehicles at a target position, respectively. This discussion is aided by numerical examples using data from hydrodynamic models and involving real operational scenarios in the coast of Portugal. Finally, in Section 5 we summarize our findings and discuss perspectives for future research.

2. TRAJECTORY OPTIMIZATION

2.1 Related Work

There is a significant amount of research on trajectory optimization for AUVs, using a variety of methods. Inanc et al. (2005) use a numerical optimal control solver to find energy and time-optimal trajectories, using a receding-horizon approach to model the time-variance of the ocean currents. The approach is improved in Zhang et al. (2008), where a fully time-varying model is used. These two works also explore the relationship between the optimal trajectories and Lagrangian Coherent Structures. Lolla et al. (2014) use a level set method to find globally time-optimal trajectories of an AUV, by tracking the boundary of the set of states reachable from a given initial state. Rhoads et al. (2010) compute the value function associated to the minimum time problem using an extremal field method, and use it to compute an optimal feedback law. Other methods discussed in the literature include nonlinear optimization (Kruger et al. (2007)) and graph search methods (Kularatne et al. (2018)).

In the above, the focus is on the case where the deployment time and position is known in advance. A dynamic programming-based method, however, produces a solution in feedback form, which allows us to compute an optimal trajectory from any initial time and position, and in turn enables the comparison of the cost values associated to different initial states.

2.2 Dynamic programming approach

Our work is focused on trajectory optimization for vehicles moving in large areas affected by time-varying currents. The approach builds on the numerical solution of the Hamilton-Jacobi-Bellman equation derived from the application of the dynamic programming principle. Although our approach does not preclude the consideration of more complex vehicle models, simple models suffice for the trajectory optimization problems under consideration. This is because the optimal trajectories do not violate the dynamic constraints of the AUVs. In what follows we consider a kinematic model of the AUV's motion, as described by the differential equation

$$\dot{\boldsymbol{x}}(t) = \boldsymbol{v}(t, \boldsymbol{x}(t)) + \boldsymbol{u}(t), \tag{1}$$

where $\boldsymbol{x} \in \mathbf{R}^2$ is the vehicle's horizontal position, $\boldsymbol{v} : \mathbf{R} \times \mathbf{R}^2 \to \mathbf{R}^2$ is a vector field modeling the flow velocity and $\boldsymbol{u} : \mathbf{R} \to \mathbf{R}^2$ is the control function. The control values $\boldsymbol{u}(t)$ are bounded in (Euclidean) norm by $r > 0$, the vehicle's maximum speed.

If we consider the optimal control problem of controlling the vehicle to a closed target set $\Omega \subset \mathbf{R}^2$ in minimum time, applying the principle of optimality of dynamic programming leads to the following Hamilton-Jacobi-Bellman equation (Aguiar et al. (2018); Bardi and Capuzzo-Dolcetta (1997)):

$$r \left\| \nabla_{\boldsymbol{x}} V(t, \boldsymbol{x}) \right\| - \left(\frac{\partial V}{\partial t} + \nabla_{\boldsymbol{x}} V(t, \boldsymbol{x}) \cdot \boldsymbol{v}(t, \boldsymbol{x}) \right) = 1, \ \boldsymbol{x} \notin \Omega,$$
$$V(t, \boldsymbol{x}) = 0, \ \boldsymbol{x} \in \Omega.$$

Here V is the value function associated to the optimal control problem, i.e., $V(t, \boldsymbol{x})$ is equal to the minimum time taken to reach the target set if the vehicle is deployed from position $\boldsymbol{x}$ at time t. If V is known, the optimal control can be computed in feedback form:

$$\boldsymbol{u}^\star(t, \boldsymbol{x}) = -r \frac{\nabla_{\boldsymbol{x}} V(t, \boldsymbol{x})}{\left\| \nabla_{\boldsymbol{x}} V(t, \boldsymbol{x}) \right\|} \tag{2}$$

This feedback law can be used directly, or one can precompute trajectories which are used as references for the vehicle's motion control system, by substituting (2) for $\boldsymbol{u}$ in (1) and integrating until the target set is reached.

In most cases, obstacles such as land regions must be included in the formulation. If the set of obstacles at time t is $\mathcal{K}(t) \subset \mathbf{R}^2$, the following boundary condition is added:

$$V(t, \boldsymbol{x}) = M, \ \boldsymbol{x} \in \mathcal{K}(t)$$

where M is a number so large that if the vehicle takes M units of time to reach the target when it departs from $\boldsymbol{x}$ at time t, the target is considered unreachable from that initial condition (e.g., it suffices to set M larger than the length of the time window considered for the mission).

2.3 Computation

We use a parallel C++ implementation of a fast sweeping algorithm to compute a numerical approximation of the value function V over a discrete grid of time-position values. The implementation is open source and available at `https://github.com/mcpca/marlin`, and to the best of our knowledge is the first publicly available implementation of a numerical method of this type. For more details see Aguiar et al. (2019).

3. MISSION PLANNING

In this and the following section, we consider AUV missions in the estuary of the Sado in Portugal (Figure 1). We use a numerical model of the currents for the region, which outputs a map of the velocity vectors defined over a curvilinear spatial grid with an average resolution of 100 meters. The velocity is calculated with a 10 minute sampling period. The velocity field models the behavior of the estuarine flow for a twelve day period starting September 10th, 2018. For a thorough description of the hydrodynamic model used to produce the data used in the results presented in this paper, see Aguiar et al. (2018) and Ribeiro et al. (2016).

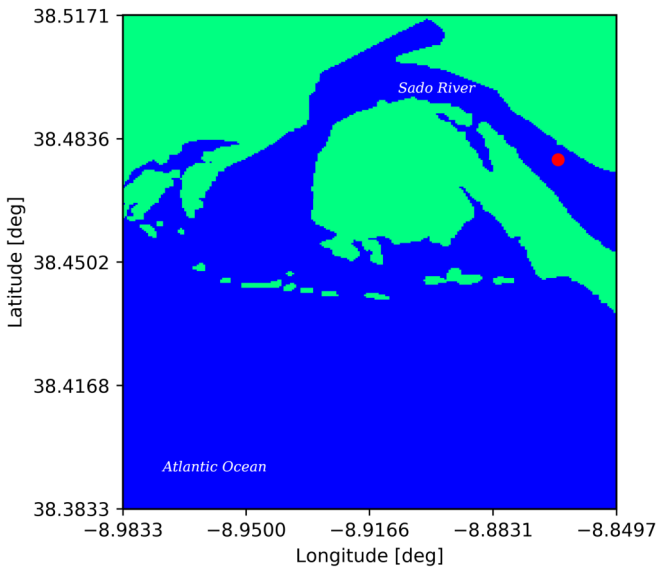

Fig. 1. Operational area for the numerical examples

The operational area is depicted in Figure 1. Land and shallow areas through which the AUV cannot navigate are included as obstacles in the formulation, and are shown in green in Figure 1. The AUV is to be deployed somewhere outside the estuary, and the target set is a 100 meter radius sphere around the point marked in red in Figure 1. Since the flow in this region is tidal-driven and the vehicle must go up the river in order to reach the target, we compute the value function using the flow values for a 12 hour period starting at low tide.

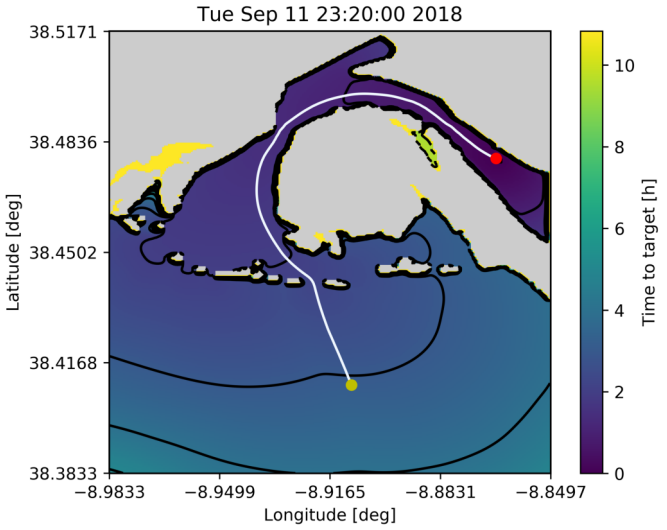

Fig. 2. Contours of the value function

One way to visualize the value of the cost at each point over the operational area is to plot the spatial contours of the value function, that is, the contours of $V(t,\cdot)$ for fixed values of t. This is exemplified in Figure 2, which shows the spatial contours of the value function at an instant of time one hour and ten minutes past low tide (the UTC time is indicated in the figure title). An optimal trajectory deployed from the yellow circle at this instant of time is plotted in white. The black lines are the level curves $V(t,\cdot) = T,\ T = 0\text{ h}, 1\text{ h}, \ldots$. When the deployment time is known in advance, these maps can be used to plan the deployment position of the vehicle. However, when the deployment time is not predetermined, this requires us to inspect these contours for all considered values of the deployment time, and compare initial states across different cost maps, which is cumbersome. We would ideally like to have the information relevant for mission planning condensed into a single time-invariant scalar field, as that is easiest for visualization.

If the vehicle is to be deployed at $\boldsymbol{x}$, we can calculate the optimal time for deploying the vehicle by minimizing $V(\cdot,\boldsymbol{x})$:

$$t^\star(\boldsymbol{x}) := \arg\min_t V(t,\boldsymbol{x})$$

This is a scalar field defined over the set of all departure positions. If there are any a priori constraints on the deployment time, these can be taken into account by only including the acceptable values of t in the minimization.

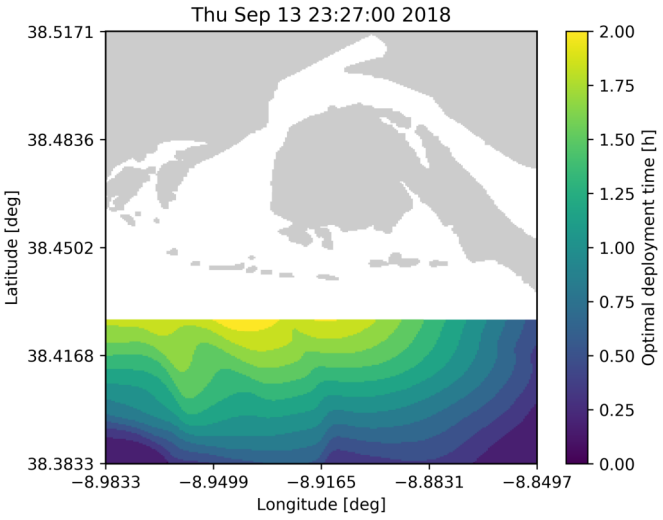

Fig. 3. Optimal deployment time

As an example, Figure 3 shows the optimal deployment time over a subset of the operational area using the values of the flow for the tide period starting at September 13th, 23:27:00 UTC. The color indicates the optimal deployment time relative to that instant of time in hours. Note that the values of the deployment time range over a finite set because the value function is known only at a discrete set of time instants.

Assuming that a vehicle deployed at the initial position $\boldsymbol{x}$ is always deployed at the corresponding optimal time $t^\star(\boldsymbol{x})$, the time variable is eliminated from the equation, and we can compare deployment positions as follows. If μ is a function which assigns to each initial state $(t,\boldsymbol{x})$ a real number $\mu(t,\boldsymbol{x})$ which is an indicator of the quality of the trajectory departing from the initial state $(t,\boldsymbol{x})$, we can obtain a time-invariant scalar map by computing $\mu^\star(\boldsymbol{x}) := \mu(t^\star(\boldsymbol{x}),\boldsymbol{x})$. The simplest choice of a metric is the value function itself, i.e. $\mu(t,\boldsymbol{x}) = V(t,\boldsymbol{x})$. The $\mu^\star$ map corresponding to this metric, for the example of Figure 3, is shown in Figure 4.

Another interesting choice of μ is

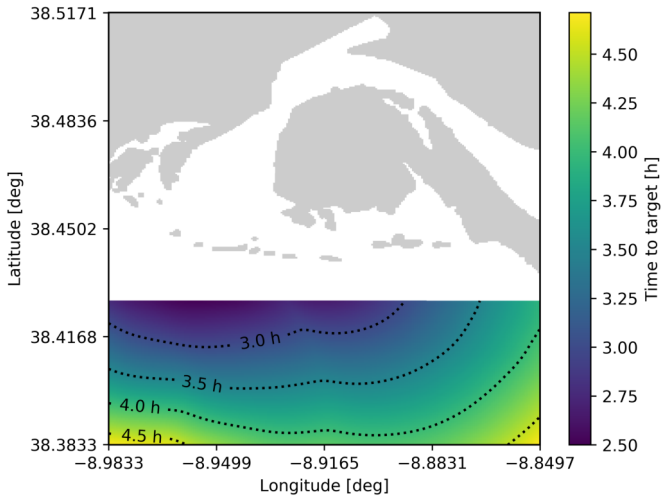

Fig. 4. Optimal time to target

$$\mu(t, \boldsymbol{x}) = \frac{s(t, \boldsymbol{x})}{rV(t, \boldsymbol{x})} - 1,$$

where $s(t, \boldsymbol{x})$ denotes the path length of the optimal trajectory departing from the initial state $(t, \boldsymbol{x})$. Since the trajectories are computed by numerically integrating (1), and hence approximated by a sequence of discrete states, s can be computed by simply summing the distances between consecutive positions. Note that the denominator, $rV(t, \boldsymbol{x})$, is equal to the distance that the vehicle travels (at nominal speed r) in an amount of time equal to the optimal mission duration. Hence, $\mu(t, \boldsymbol{x})$ can be seen as the gain in the vehicle's average velocity along the trajectory, describing how much the vehicle benefited from the flow velocity when departing from $(t, \boldsymbol{x})$. Naturally, μ may take on negative values at initial states from which the vehicle will face opposing current velocities.

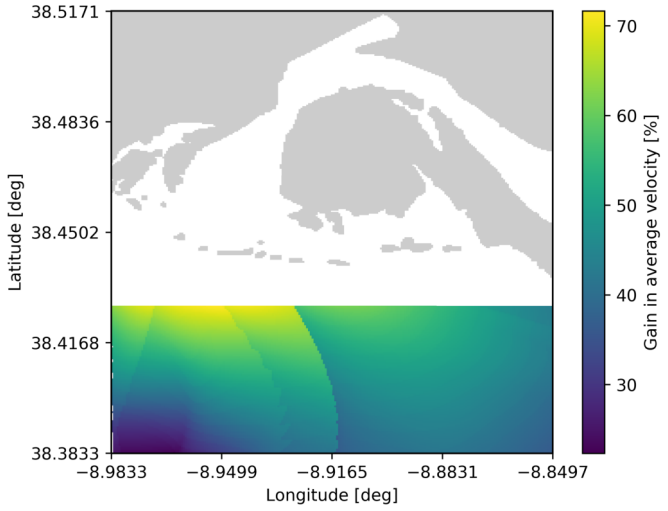

Fig. 5. Gain in the average velocity

This is exemplified in Figure 5, using the same value function as in Figure 3. There are several discontinuities in the map which divide regions where the optimal trajectories go through different sides of the same obstacles, which is not visible in any of the other plots.

4. OPTIMAL TIME RENDEZVOUS

We now illustrate how the value function corresponding to the minimum time control problem can be used to plan a rendezvous between two or more vehicles. Specifically, we consider the problem of finding a trajectory for each vehicle such that all the vehicles arrive at a target location at the same time. We discuss how the value function can be used to find the feasible deployment times and locations for each vehicle, assuming that the deployment time and location of one of the vehicles are fixed a priori.

For simplicity and clarity of presentation, we focus on the two vehicle case, and assume that the two vehicles travel at the same nominal speed r. In this case, a single computation of the minimum time to reach the target is sufficient for obtaining optimal trajectories which lead the two vehicles to arrive at the target approximately at the same time. When the two vehicles travel at different nominal speeds, what follows still applies, but with a different value function for each vehicle. The operational area and target set are the same as in the previous section. Let $\boldsymbol{x}_i$ and t_i be the deployment position and time of the ith vehicle, respectively, where $i = 1, 2$. We henceforth assume that t_1 and $\boldsymbol{x}_1$ have been chosen a priori, e.g. via the methods described in the previous section.

If we assume that the two vehicles are deployed at the same time, i.e. $t_2 = t_1$, then in order to have the two vehicles arrive simultaneously at the target we should have

$$V(t_1, \boldsymbol{x}_2) = V_1$$

where $V_1 := V(t_1, \boldsymbol{x}_1)$, i.e., $\boldsymbol{x}_1$ and $\boldsymbol{x}_2$ should lie on the same level set of $V(t_1, \cdot)$. An example is shown in Figure 6. If the first vehicle is deployed from the position marked in yellow, the second vehicle can be deployed from any of the positions along the black dashed curve in order to arrive at the target position (the red point) simultaneously. (Note that this formulation does not include provisions to preclude collisions.)

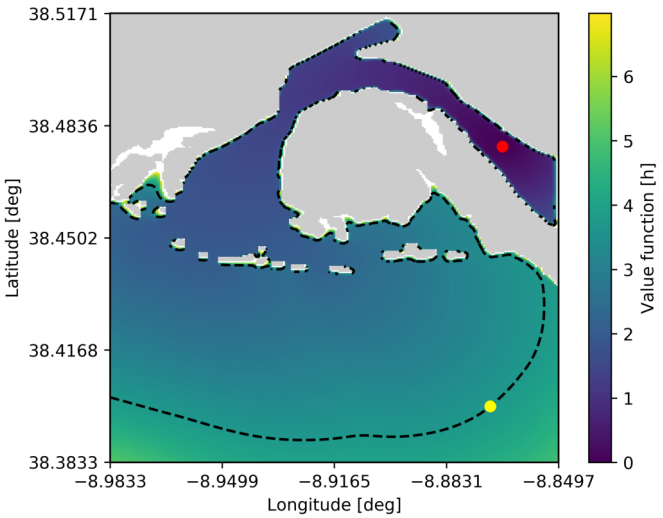

Fig. 6. Set of feasible deployment positions for timed rendezvous when the vehicles are deployed at the same instant of time.

In practice, the arrival times will not be exactly the same. If we specify instead that the two vehicles arrive at the

target within ε units of time of each other, then $\boldsymbol{x}_2$ should be chosen from the set

$$\{\boldsymbol{x} \mid |V_1 - V(t_1, \boldsymbol{x})| \leq \varepsilon\}.$$

An example is shown in Figure 7. The shaded region indicates the set of positions the second vehicle may be deployed from in order to have the two vehicles arrive within fifteen minutes of each other, when the first vehicle is deployed from the position indicated by the yellow dot.

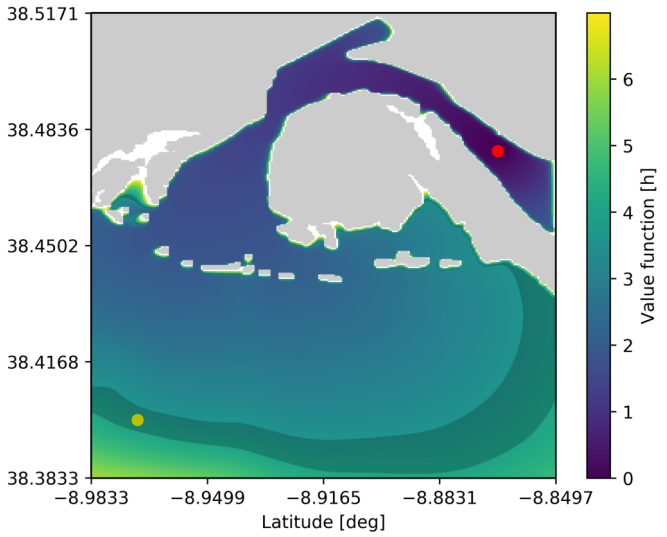

Fig. 7. Set of feasible deployment positions for approximate rendezvous

When the deployment time of the second vehicle is not necessarily equal to t_1, $\boldsymbol{x}_2$ and t_2 should jointly satisfy the equation

$$t_1 + V_1 = t_2 + V(t_2, \boldsymbol{x}_2), \tag{3}$$

i.e., the arrival times should be equal. If t_2 is fixed, the set of feasible deployment positions is again a single level curve of the value function, $\{\boldsymbol{x} \mid V(t_2, \boldsymbol{x}) = t_1 + V_1 - t_2\}$, so the selection of the deployment position can be made in a way similar to the above (assuming that this set is nonempty). When t_2 is not fixed, we can use the following approach: for each $\boldsymbol{x}_2$ compute

$$t^r(\boldsymbol{x}_2) := \arg \min_{t \in \mathcal{A}(\boldsymbol{x}_2)} |t_1 + V_1 - t - V(t, \boldsymbol{x}_2)|, \tag{4}$$

i.e., $t^r(\boldsymbol{x}_2)$ is the deployment time which leads to the least absolute difference in the arrival time of the two vehicles. Here $\mathcal{A}(\boldsymbol{x}_2) = \{t : V(t, \boldsymbol{x}_2) < M\}$, where M is as in section 2.2. Any a priori restrictions on the deployment time can be taken into account by further restricting the set of t over which the minimization is performed. If for a particular value of $\boldsymbol{x}_2$ there are multiple solutions to the minimization (4), some other criterion must be used to choose t^r from among those solutions. The function t^r is analogous to the function $t^\star$ of the previous section. An example computation of t^r is shown in Figure 8. The deployment position of the first vehicle is indicated by the yellow circle and the colors indicate the optimal deployment time relative to the start of the time window considered in the computation of the value function.

Figure 9 shows an example of the trajectories generated for two vehicles using this method. The trajectory shown in blue corresponds to the trajectory of a vehicle deployed

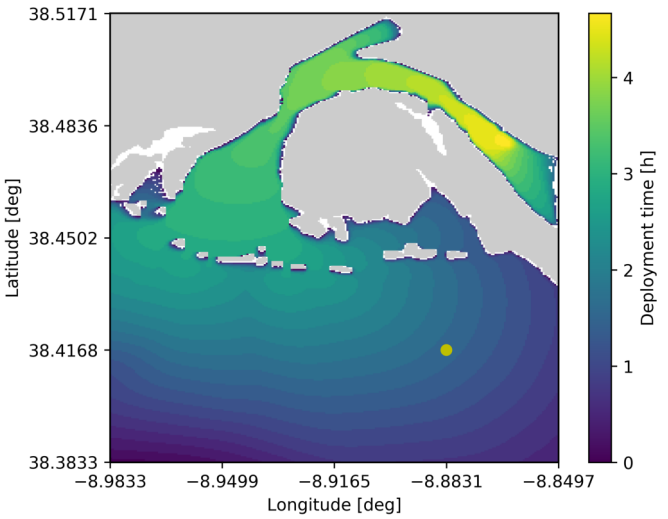

Fig. 8. The optimal deployment time for timed rendezvous of two vehicles as a function of the deployment position

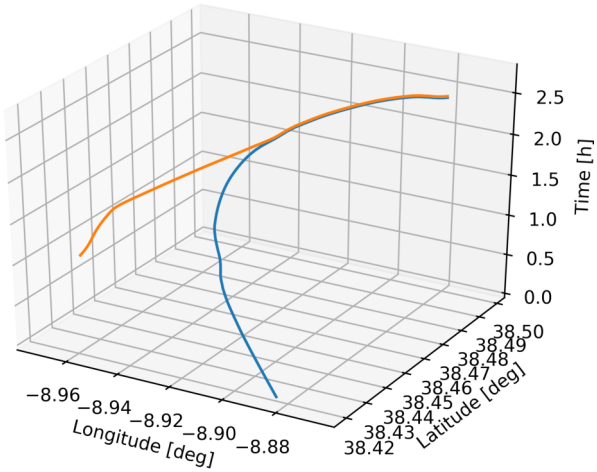

Fig. 9. Trajectories for rendezvous of two vehicles

from the position indicated by the yellow circle in Figure 8, and the deployment time for the second vehicle was selected using the map shown in that figure. Note that the trajectories coincide after a certain point; several approaches can be employed to deal with this problem, such as having the vehicles navigate at different depths, or coordinated operation of the AUVs (see, e.g., Jan H. van Schuppen (2014)). A thorough treatment of this problem is outside the scope of this paper.

In the case of n vehicles, if the value function of the ith vehicle is V_i and $(t_1, \boldsymbol{x}_1)$ is fixed, the condition on each $(t_i, \boldsymbol{x}_i)$ is

$$t_i + V_i(t_i, \boldsymbol{x}_i) = t_1 + V_1(t_1, \boldsymbol{x}_1).$$

5. CONCLUSIONS

We explored the use of the value function associated to minimum time optimal control problems involving unmanned underwater vehicles operating under the influence of currents. This is done for a realistic setting, where the

time-varying values of the currents are obtained from state of the art prediction models. In particular, we showed how the value function can be used to plan the optimal deployment time and location of the vehicle, and how it can be used to plan a two vehicle mission where the two vehicles should arrive at a target set at the same time.

In the first problem, we focused on the case where the deployment time is not fixed in advance. The cost-to-go depends on the initial position and on the deployment time, making it hard to compare the cost of several candidate deployment positions. Our approach is to first compute the optimal deployment time as a function of the deployment position, and then compare deployment positions with the understanding that the vehicle will be deployed at the optimal time associated to its deployment position. This eliminates the time variable and allows us to compare candidate deployment positions in terms of their cost or other scalar functions of the optimal trajectory associated to each initial state.

In the second problem, assuming that the deployment time and position of one of the vehicles is fixed, we showed how the value function can be used to plan the deployment position of a second vehicle. When the deployment time of the second vehicle is not fixed, an approach similar to the one taken for the first problem once again allows us to focus on choosing the deployment position.

Although our mission examples focused on autonomous underwater vehicles, the ideas presented in this paper are largely independent of the type of vehicle or the medium through which it travels, and should be useful whenever there is a time-varying factor (in the case of our examples, the current velocity) which can have a meaningful impact on mission planning decisions.

A possible direction for further research is the application of similar techniques in multi-stage missions. In the case of underwater vehicles under the influence of currents, the deployment depth, which was not considered here, could also play a significant role when the flow has considerable vertical variability.

ACKNOWLEDGEMENTS

This work was partially funded by project ENDURANCE – Sistema baseado em veículos autónomos para observação oceanográfica de longa duração, funded by Norte Portugal Regional Operational Programme (NORTE 2020), under the PORTUGAL 2020 Partnership Agreement, through the European Regional Development Fund (ERDF), and by the EUMarineRobots project, funded by the European Union's Horizon 2020 research and innovation programme under grant agreement no. 731103. R. M. benefits from a Post-Doctoral grant (SFRH/BPD/115093/2016) given by the Portuguese Science Foundation (FCT).

REFERENCES

Aguiar, M., de Sousa, J.B., Dias, J.M., da Silva, J.E., Mendes, R., and Ribeiro, A.S. (2018). Trajectory optimization for underwater vehicles in time-varying ocean flows. In *2018 IEEE/OES Autonomous Underwater Vehicle Workshop (AUV)*. IEEE. doi:10.1109/auv.2018.8729777.

Aguiar, M., de Sousa, J.B., Dias, J.M., da Silva, J.E., Mendes, R., and Ribeiro, A.S. (2019). Optimizing autonomous ocean vehicle routes with the aid of high resolution ocean models. In *OCEANS 2019 MTS/IEEE Seattle*. IEEE.

Bardi, M. and Capuzzo-Dolcetta, I. (1997). *Optimal Control and Viscosity Solutions of Hamilton-Jacobi-Bellman Equations*. Birkhäuser Boston. doi:10.1007/978-0-8176-4755-1.

Bellingham, J.G. and Rajan, K. (2007). Robotics in remote and hostile environments. *Science*, 318(5853), 1098–1102. doi:10.1126/science.1146230.

Bellman, R. (1954). The theory of dynamic programming. *Bull. Amer. Math. Soc.*, 60(6), 503–515.

Ferreira, A.S., Costa, M., Py, F., Pinto, J., Silva, M.A., Nimmo-Smith, A., Johansen, T.A., de Sousa, J.B., and Rajan, K. (2018). Advancing multi-vehicle deployments in oceanographic field experiments. *Autonomous Robots*, 43(6), 1555–1574. doi:10.1007/s10514-018-9810-x.

Inanc, T., Shadden, S., and Marsden, J. (2005). Optimal trajectory generation in ocean flows. In *Proceedings of the 2005, American Control Conference, 2005.* IEEE. doi:10.1109/acc.2005.1470035.

Jan H. van Schuppen, T.V. (ed.) (2014). *Coordination Control of Distributed Systems*, volume 456 of *Lecture Notes in Control and Information Sciences*. Springer, Cham.

Kruger, D., Stolkin, R., Blum, A., and Briganti, J. (2007). Optimal AUV path planning for extended missions in complex, fast-flowing estuarine environments. In *Proceedings 2007 IEEE International Conference on Robotics and Automation*. IEEE. doi:10.1109/robot.2007.364135.

Kularatne, D., Bhattacharya, S., and Hsieh, M.A. (2018). Going with the flow: a graph based approach to optimal path planning in general flows. *Autonomous Robots*, 42(7), 1369–1387. doi:10.1007/s10514-018-9741-6.

Lolla, T., Haley, P.J., and Lermusiaux, P.F.J. (2014). Time-optimal path planning in dynamic flows using level set equations: realistic applications. *Ocean Dynamics*, 64(10), 1399–1417. doi:10.1007/s10236-014-0760-3.

Rhoads, B., Mezic, I., and Poje, A. (2010). Minimum time feedback control of autonomous underwater vehicles. In *49th IEEE Conference on Decision and Control (CDC)*. IEEE. doi:10.1109/cdc.2010.5717533.

Ribeiro, A.S., Sousa, M.C., e Silva, J.D.L., and Dias, J.M. (2016). David and goliath revisited: Joint modelling of the tagus and sado estuaries. *Journal of Coastal Research*, 75(sp1), 123–127. doi:10.2112/si75-025.1.

Wynn, R.B., Huvenne, V.A., Bas, T.P.L., Murton, B.J., Connelly, D.P., Bett, B.J., Ruhl, H.A., Morris, K.J., Peakall, J., Parsons, D.R., Sumner, E.J., Darby, S.E., Dorrell, R.M., and Hunt, J.E. (2014). Autonomous underwater vehicles (AUVs): Their past, present and future contributions to the advancement of marine geoscience. *Marine Geology*, 352, 451–468. doi:10.1016/j.margeo.2014.03.012.

Zhang, W., Inanc, T., Ober-Blobaum, S., and Marsden, J.E. (2008). Optimal trajectory generation for a glider in time-varying 2d ocean flows b-spline model. In *2008 IEEE International Conference on Robotics and Automation*. IEEE. doi:10.1109/robot.2008.4543348.